Atom Transfer Radical Polymerization Directly from Poly(vinylidene fluoride): Surface and Antifouling Properties

YIWANG CHEN,[1,2] DONGMEI LIU,[1] QILAN DENG,[2] XIAOHUI HE,[2] XIAOFENG WANG[2]

[1]Department of Chemistry, Nanchang University, Nanchang 330047, People's Republic of China

[2]School of Materials Science and Engineering, Nanchang University, Nanchang 330047, People's Republic of China

Received 14 February 2006; accepted 14 March 2006
DOI: 10.1002/pola.21456
Published online in Wiley InterScience (www.interscience.wiley.com).

ABSTRACT: The direct preparation of grafting polymer brushes from commercial poly (vinylidene fluoride) (PVDF) films with surface-initiated atom transfer radical polymerization (ATRP) is demonstrated. The direct initiation of the secondary fluorinated site of PVDF facilitated grafting of the hydrophilic monomers from the PVDF surface. Homopolymer brushes of 2-(*N*,*N*-dimethylamino)ethyl methacrylate (DMAEMA) and poly (ethylene glycol) monomethacrylate (PEGMA) were prepared by ATRP from the PVDF surface. The chemical composition and surface topography of the graft-functionalized PVDF surfaces were characterized by X-ray photoelectron spectroscopy, attenuated total reflectance/Fourier transform infrared spectroscopy, and atomic force microscopy. A kinetic study revealed a linear increase in the graft concentration of poly[2-(*N*,*N*-dimethylamino)ethyl methacrylate] (PDMAEMA) and poly[poly(ethylene glycol) monomethacrylate] (PPEGMA) with the reaction time, indicating that the chain growth from the surface was consistent with a controlled or living process. The living chain ends were used as macroinitiators for the synthesis of diblock copolymer brushes. The water contact angles on PVDF films were reduced by the surface grafting of DMAEMA and PEGMA. Protein adsorption experiments revealed a substantial antifouling property of PPEGMA-grafted PVDF films and PDMAEMA-grafted PVDF films in comparison with the pristine PVDF surface. J Polym Sci Part A: Polym Chem 44: 3434–3443, 2006

Keywords: atom transfer radical polymerization (ATRP); contact angle; fluoropolymers; graft copolymers; poly(vinylidene fluoride); protein antifouling

INTRODUCTION

Fluoropolymers, such as poly(vinylidene fluoride) (PVDF), constitute one of the most important families of engineering polymers. They are well known for their physical and chemical resistance.[1–3] In addition to numerous and versatile industrial applications, new developments of PVDF have been found in biotechnology[4–7] and in the biomedical sector (vascular sutures and regeneration templates).[8–10] However, biomedical equipment is subject to significant nonspecific protein adsorption because of the low surface energy and hydrophobicity of PVDF. To improve the surface hydrophilicity of PVDF, a large amount of work has been devoted to the surface

Correspondence to: Y. Chen (E-mail: ywchen@ncu.edu.cn)
Journal of Polymer Science: Part A: Polymer Chemistry, Vol. 44, 3434–3443 (2006)

modification of fluoropolymers by chemicals,[11] plasma,[12–14] irradiation,[15] corona discharge,[16] flame,[17] ozone treatment,[18] and vacuum ultraviolet radiation.[19,20] The surface modification of polymers via molecular design is one of the most versatile approaches to imparting new functionalities, such as improved hydrophilicity, biocompatibility, conductivity, and lubricative and adhesive properties, to the existing polymers.[21–23] Recently, much attention has been centered on the modification of fluoropolymers via surface graft copolymerization or surface-initiated polymerization.[2,24–30]

Progress in polymerization has made it possible to produce polymer chains or brushes on a surface with a controlled length and structure.[21,31,32] Polymers of various architectures (block, comb, graft, hyperbranched, star, etc.) have been synthesized by living radical polymerizations. Successful examples of living radical polymerization include nitroxide-mediated radical polymerization,[33] atom transfer radical polymerization (ATRP),[34,35] and reversible addition–fragmentation chain transfer polymerization.[36] ATRP does not require stringent experimental conditions, as in the case of cationic and anionic polymerization. The preparation of well-defined polymer brushes via surface-initiated living radical polymerization has also received a considerable amount of attention in recent years.[37–55] ATRP has recently been used to prepare graft copolymers from polymeric macroinitiators, polymer chains with regularly spaced, pendant chemical groups containing radically transferable halogen atoms.[56,57] The halogen atoms serve as initiation sites for the polymerization of side chains by ATRP. A number of high-volume commercial polymers, including poly (vinyl chloride) (PVC), PVDF, and chlorinated polyolefins, comprise repeat units with secondary halogen atoms pendant. In principle, these polymers might be used as ATRP macroinitiators for the preparation of functionalized derivatives. However, it has been reported that the secondary chlorine atoms of PVC are too strongly bonded to serve as ATRP initiation sites.[58] Hester et al.[59] demonstrated the direct preparation of amphiphilic graft copolymers having PVDF backbones by the ATRP of hydrophilic side chains initiated at the secondary halogenated sites of PVDF.

In this work, surface modifications of PVDF films with well-defined polymer brushes by direct surface-initiated ATRP from the secondary halogenated sites on the surface are demonstrated. Homopolymer brushes of poly[2-(*N,N*-dimethylamino)ethyl methacrylate] (PDMAEMA) and poly [poly(ethylene glycol) monomethacrylate] (PPEGMA) were prepared by ATRP from secondary fluorine atoms on the PVDF surface. Diblock copolymer brushes were prepared with the homopolymer brushes as the macroinitiators for the ATRP of the second monomer. The chemical composition and surface topography of the nontreated and graft-functionalized PVDF surfaces were determined by X-ray photoelectron spectroscopy (XPS), attenuated total reflectance (ATR)/Fourier transform infrared (FTIR) spectroscopy, and atomic force microscopy (AFM). The hydrophilic property and antifouling property of PPEGMA-grafted PVDF surfaces were characterized by contact-angle measurement and XPS analysis.

EXPERIMENTAL

Materials

PVDF films with a thickness of 0.5 mm were obtained from Goodfellow Cambridge, Ltd. (Huntingon, England). The PVDF films were sliced into rectangular strips (ca. 1 cm $\times$ 2 cm). To remove the organic residues on the surface, the PVDF films were washed with acetone, methanol, and doubly distilled water in that order. The films were dried under reduced pressure at room temperature for about 24 h and then stored in a clean and dry box. Poly(ethylene glycol) monomethacrylate (PEGMA) macromonomer [number-average molecular weight (M_n) = 300] and 2-(*N,N*-dimethylamino)ethyl methacrylate (DMAEMA) were passed through an inhibitor-remover column to remove the inhibitors and then stored in clean vessels at -10 °C. Styrene (St) was distilled under reduced pressure and stored in an argon atmosphere at -10 °C. Copper(I) bromide and copper(I) chloride were purified according to procedures described in the literature.[39] 2,2-Bipyridine (bpy), ethyl bromoisobutyrate (EBiB), 1,1,4,7, 10,10-hexamethyltriethylenetetramine (HMTETA), and other chemical reagents were used without further purification.

Surface Characterization

ATR–FTIR spectra of the surface-functionalized films were obtained with a Shimadzu IR Prestige 21 spectrophotometer with a ZnSe prism with an incident angle of 60°. Each spectrum was collected by the accumulation of 160 scans at a reso-

lution of 4 cm^{-1}. A JC2000A contact-angle measurer was used to measure the static water contact angles of the polymer films at 25 °C and 60% relative humidity with a sessile drop method. For each angle reported, at least five sample readings from different surface locations were averaged. The value was read within 1 min after the water drop was placed on the surface. The reported angles were reliable to ±1°. Gel permeation chromatography measurements were carried out with a Waters 1515 high-performance liquid chromatograph equipped with a Styragel mixed-C column and a Waters 2414 refractive-index detector. *N, N*-Dimethylformamide was used as the mobile phase. Monodispersed polystyrene (PSt) standards (Aldrich Chemical Co.) were used to generate the calibration curve.

The chemical compositions of the nontreated and functionalized PVDF surfaces were determined by XPS. The XPS measurements were performed on a Kratos Axis Ultra spectrometer with a monochromatic Al Kα X-ray source (1486.71 eV photons) at a constant dwelling time of 100 ms and a pass energy of 40 eV. The samples were mounted on standard sample studs by means of double-sided adhesive tape. The core-level signals were obtained at a photoelectron takeoff angle (measured with respect to the sample surface) of 90°. The X-ray source was run at a reduced power of 225 W (15 kV and 15 mA). The pressure in the analysis chamber was kept at 8–10 Torr or lower during each measurement. All binding energies (BEs) were referenced to the C 1s hydrocarbon peak at 284.8 eV. Surface elemental stoichiometries were determined from the spectral area ratios, after correction with the experimentally determined sensitivity factors, and were reliable to within ±10%. The elemental sensitivity factors were calibrated with stable binary compounds of well-established stoichiometries.

The topography of the pristine and graft-polymerized PVDF surfaces was studied by AFM with an AJ-III atomic force microscope from Shanghai AJ Nano-Science Development Co., Ltd. In each case, a square area of 5 μm × 5 μm was scanned with the tapping mode. The drive frequency was 330 ± 50 kHz, and the voltage was between 3 and 4.0 V. The drive amplitude was about 300 mV, and the scanning rate was 0.5–1.0 Hz. An arithmetic mean of the surface roughness was calculated from the roughness profile determined by AFM with the implemented algorithms.

The thickness of the polymer films grafted on the PVDF substrates was determined by ellipsometry. The measurements were carried out on a variable-angle spectroscopic ellipsometer (M-2000, J. A. Woollam, Inc., Lincoln, NE) at incident angles of 60 and 65° in the wavelength range of 370–1000 nm. The refractive index of the dried films at all wavelengths was assumed to be 1.52. The refractive index of the PVDF substrate was set to be 1.42. All measurements were conducted in dry air at room temperature. For each sample, thickness measurements were made on at least three different surface locations. Each reported thickness was reliable to ±1 nm. Data were recorded and processed with the WVASE32 software package.

Direct Surface-Initiated ATRP

PPEGMA-Grafted PVDF Surface

For the preparation of PPEGMA brushes on PVDF surfaces, PEGMA (1.5 mL, 4.5 mmol), CuCl (4.5 mg, 0.045 mmol), $CuCl_2$ (1.26 mg, 0.009 mmol), and bpy (17 mg, 0.108 mmol) were added to 1 mL of doubly distilled water. The mixture was stirred and purged with argon for 30 min. The pristine PVDF substrate was then introduced into the solution. The reaction flask was sealed and placed in a 31 °C water bath for a predetermined period. After the reaction, the PVDF substrate with surface-grafted PPEGMA (the PVDF-*g*-PPEGMA surface) was removed from the reaction mixture and extracted thoroughly with excess ethanol and doubly distilled water over 10 h.

PDMAEMA-Grafted PVDF Surface

For the preparation of poly[2-(*N,N*-dimethylamino) ethyl methacrylate (PDMAEMA) brushes on PVDF surfaces, DMAEMA (3.25 mL, 19.5 mmol), CuBr (13.2 mg, 0.09 mmol), and HMTETA (24.6 μL, 0.09 mmol) were added to 3 mL of tetrahydrofuran. The solution was degassed with argon for 20 min. The pristine PVDF substrate and the free initiator, EBiB (13.2 μL, 0.09 mmol), were then added to the solution. The reaction flask was sealed and kept in a 65 °C oil bath for a predetermined period. After the reaction, the PVDF substrate with surface-grafted PDMAEMA (the PVDF-*g*-PDMAEMA surface) was removed from the solution and extracted thoroughly with excess ethanol for 24 h. The reaction solution was washed through a silicon column with excess ethanol to get rid of copper(II). Then, the free PDMAEMA that formed in the solution by the

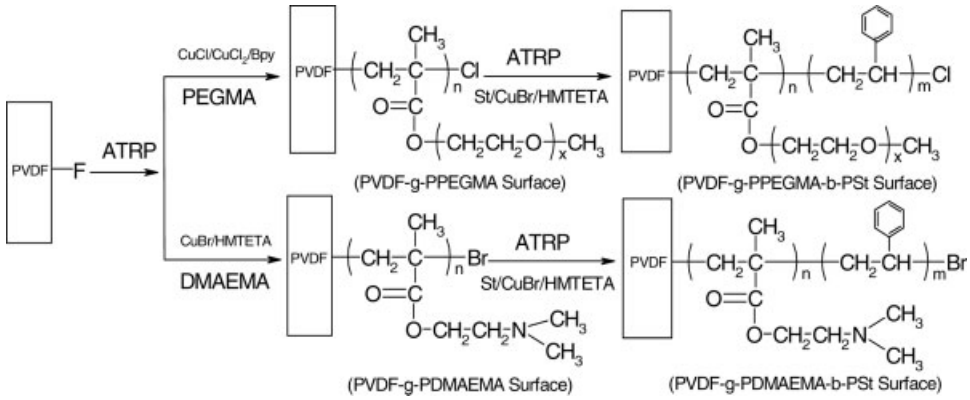

Scheme 1. Schematic diagram illustrating the processes of direct surface-initiated ATRP from the PVDF surface and block polymerization from the polymer-grafted PVDF surface.

free initiator was recovered by precipitation in excess petroleum. The monomer conversion was determined gravimetrically.

Diblock Copolymer Brushes on PVDF Surfaces

For the preparation of PSt blocks from the PVDF-*g*-PPEGMA and PVDF-*g*-PDMAEMA surfaces, St (3.46 mL, 30.0 mmol), CuBr (14.4 mg, 0.1 mmol), and HMTETA (27.2 μL, 0.1 mmol) were added to 2 mL of a mixed solvent (1:1 v/v anisole/acetonitrile). The solution was degassed with argon for 30 min. The previously prepared PVDF-*g*-PPEGMA substrate (or PVDF-*g*-PDMAEMA substrate) and the free initiator, EBiB (14.4 μL, 0.1 mmol), were then added to the solution. The reaction flask was sealed and placed in a 110 °C oil bath for 24 h. After the reaction, the PVDF surface grafted with PPEGMA-*b*-PSt (or PDMAEMA-*b*-PSt) diblock copolymer brushes (the PVDF-*g*-PPEGMA-*b*-PSt or PVDF-*g*-PDMAEMA-*b*-PSt surface) was removed from the solution and extracted thoroughly with excess toluene for 24 h to remove any adhered monomer and homopolymer. The free PSt that formed in the solution by the free initiator was recovered by precipitation in excess methanol.

Protein Fouling Measurements

To investigate the antifouling properties of the PVDF-*g*-PPEGMA surfaces, the PVDF-*g*-PPEGMA surfaces were first exposed to solutions containing bovine serum albumin (BSA). The PVDF-*g*-PPEGMA surfaces were hydrated initially by immersion in methanol, which was followed by immersion in distilled water. The PVDF-*g*-PPEGMA surfaces were subsequently washed with 0.01 M phosphate buffer saline (PBS; pH 7.4) for 1 h before being incubated in PBS containing 2 mg/mL of BSA for 24 h at room temperature. After removal from the protein solution, they were washed for 5 min in three batches of PBS, which were followed by three batches of distilled water. Finally, the samples were dried in a vacuum oven at room temperature. The surface coverage of BSA was quantified by XPS, with the nitrogen signal associated with BSA. Survey spectra were run in the BE range of 0–1000 eV. The near-surface atomic compositions of the surfaces were determined from the numerically integrated core-level spectral area ratios, which were corrected with the respective elemental sensitivity factors.

RESULTS AND DISCUSSION

Direct Surface-Initiated ATRP on PVDF Surfaces

Because Hester et al.[59] demonstrated the direct preparation of amphiphilic graft copolymers having PVDF backbones by ATRP initiated at the secondary halogenated sites of PVDF, the preparation of polymer brushes on PVDF surfaces by direct surface-initiated ATRP was attempted in this work (Scheme 1). The presence of the grafted polymer on PVDF surfaces was ascertained first by ATR–FTIR spectra. The ATR–FTIR spectra of the PVDF-*g*-PPEGMA and PVDF-*g*-PDMAEMA surfaces reveal the appearance of the absorption band at 1732 cm^{-1}, which is attributable to the stretching of the ester carbonyl group, as shown in Figures 1 and 2, respectively. The variations of

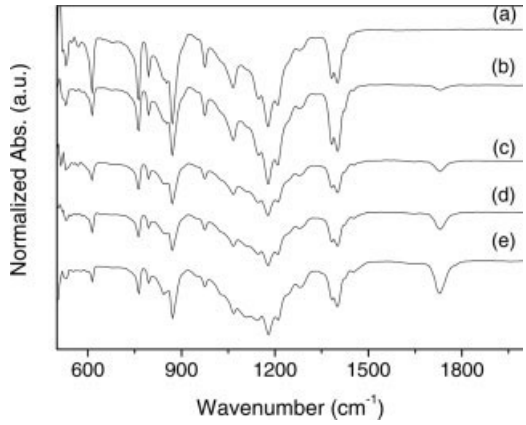

Figure 1. ATR–FTIR spectra of (a) the pristine PVDF surface and (b–e) the PVDF surface PPEGMA-grafted for 5, 8, 11, and 14 h, respectively (reaction conditions: [PEGMA]/[CuCl]/[$CuCl_2$]/[bpy] = 100:1:0.2:2.4; [PEGMA] = 1.8 M; solvent = water; temperature = 31 °C).

the graft concentration are reflected in the changes in the ratio of the intensity of the absorption band at 1732 cm^{-1} to that of the absorption band at 1400 cm^{-1} (attributable to PVDF). For proving the ATRP initiated at the secondary halogenated sites of PVDF on the surface, comparison experiments with a polyethylene surface instead of a PVDF surface with CuCl/$CuCl_2$/bpy as a catalyst system to prepare PPEGMA brushes were carried out. Additional control experiments were performed in a solution of PEGMA and a pristine PVDF surface without CuCl/$CuCl_2$/bpy. No evidence existed from the observation of the absence of ester carbonyl at 1732 cm^{-1} in ATR–FTIR spectra of PVDF surfaces in both experiments.

The variation of the water contact angle for the PVDF surfaces with different polymer brushes indicates that the hydrophilicity of a PVDF surface can be easily tuned. The contact angle of the nontreated PVDF surface was about 93°. As shown in Figure 3, when grafted with a PPEGMA and PDMAEMA layer, the PVDF surface became more hydrophilic, and the contact angle decreased with an increase in the graft concentration (with respect to the reaction time).

As shown in Figure 4, the presence of the grafted polymer on the PVDF surface was ascertained by XPS analysis as well. The C 1s core-level spectrum of the nontreated PVDF surface consists of two peak components of about equal integral areas with BE at 286.2 eV for the CH_2 species and at 290.9 eV for the CF_2 species [Fig. 4(a)]. The peak component at 284.6 eV is attributable to the C—H species from the internal reference for the XPS scan. The C 1s core-level spectra of the PVDF-*g*-PDMAEMA surface [Fig. 4(b)] can be curve-fitted with six peak components having BEs at about 284.6, 286.2, 286.8, 287.1, 288.9, and 290.9 eV, which are attributable to the C—H species of the graft polymer, CH_2 species adjacent to CF_2, and C—N, C—O, O—C=O, and CF_2 species, respectively. The C 1s core-level spectra of the PVDF-*g*-PPEGMA surface [Fig. 4(c)] can be curve-fitted with five peak components having BEs at about 284.6, 286.2, 287.1, 288.9, and 290.9 eV, which are attributable to the C—H spe-

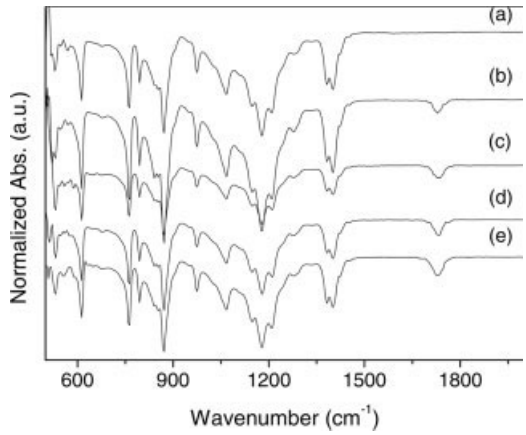

Figure 2. ATR–FTIR spectra of (a) the pristine PVDF surface and (b–e) the PVDF surface PDMAEMA-grafted for 2.5, 3, 4, and 5 h, respectively (reaction conditions: [DMAEMA]/[EBiB]/[CuBr]/[HMTETA] = 210:1:1:1; [DMAEMA] = 3.21 M; solvent = 1:1 v/v anisole/acetonitrile; temperature = 65 °C).

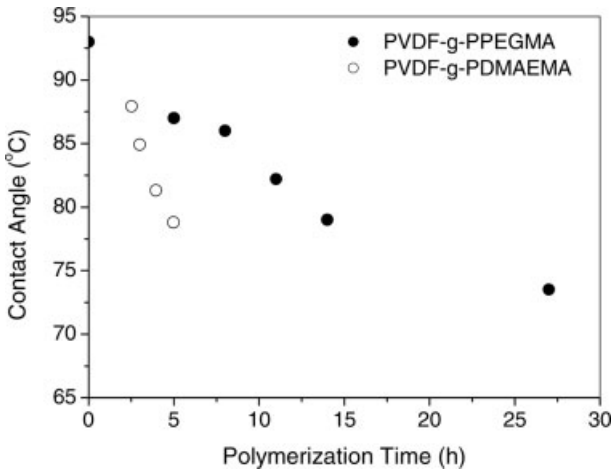

Figure 3. Variation of the water contact angle of the PVDF-*g*-PPEGMA and PVDF-*g*-PDMAEMA surfaces on the graft polymerization time of surface-initiated ATRP.

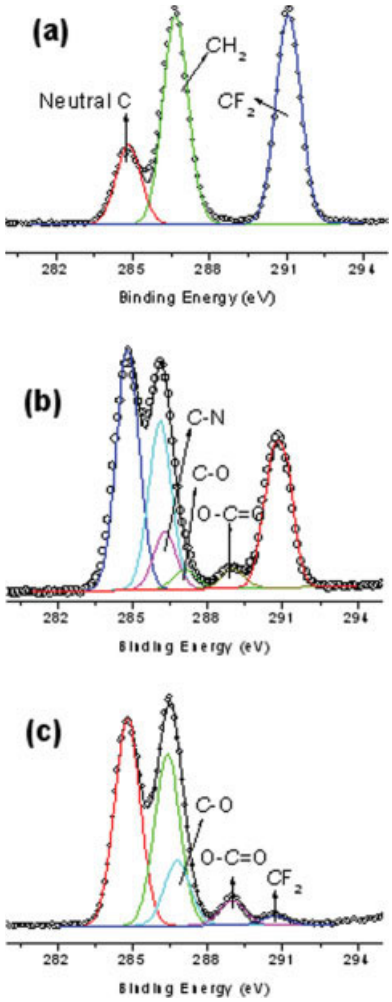

Figure 4. XPS C1s core-level spectra of (a) the pristine PVDF surface, (b) the PVDF surface with graft PDMAEMA brushes in a thickness of 3.9 nm, and (c) the PVDF surface with graft PPEGMA brushes in a thickness of 6.4 nm.

cies of the graft polymer, CH_2 species adjacent to CF_2, and C—O, O—C=O, and CF_2 species, respectively. The [C—N]/[C—O]/[O—C=O] ratios of the PVDF-*g*-PDMAEMA surface and [C—O]/[O—C=O] ratios of the PVDF-*g*-PPEGMA surface, obtained from XPS analysis, are in fairly good agreement with the respective theoretical ratios (3:1:1 and 10:1). In addition, the CF_2 peak component associated with the PVDF substrate persists in the curve-fitted C 1s core-level spectra of the PVDF-*g*-PDMAEMA and PVDF-*g*-PPEGMA surfaces but presents a lower area in comparison with the CH_2 component. The graft concentrations of the PDMAEMA and PPEGMA brushes grown on the PVDF surface can be derived from the O—C=O peak component to the CF_2 peak component. With an increase in the graft polymerization time, the [O—C=O]/[CF_2] ratio increases for both graft-functionalized PVDF surfaces until the CF_2 peak component cannot determined by XPS. This result suggests that the thickness of the grafted polymer layer is gained gradually until the thickness of the graft layer is beyond the probing depth of the XPS technique.

The evidence for controlled polymerization from the PVDF surfaces was also obtained from the free PDMAEMA formed by the free initiator. Figure 5(a) shows the linearity relationship between ln([M_0]/[M]) and time, where [M_0] is the initial monomer concentration and [M] is the monomer concentration. The result indicated that the concentration of the growing species remained constant and first-order kinetics were obtained. The observation of a fitted line through nonzero revealed that the strong BE of C—F led

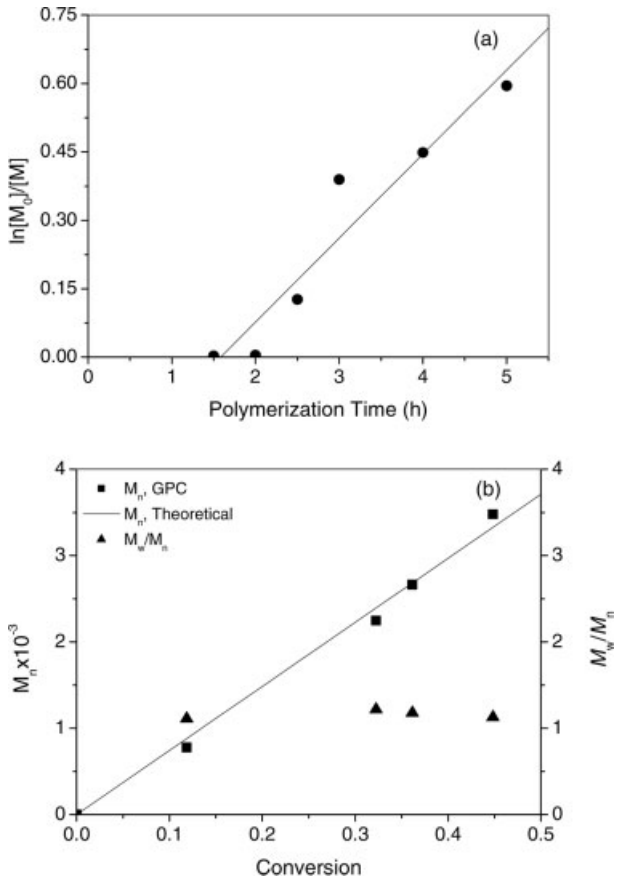

Figure 5. Relationship (a) between ln([M_0]/[M]) and the polymerization time and (b) between M_n and the monomer conversion (reaction conditions: [DMAEMA]/[EBiB]/[CuBr]/[HMTETA] = 210:1:1:1; [DMAEMA] = 3.21 M; solvent = 1:1 v/v anisole/acetonitrile; temperature = 65 °C).

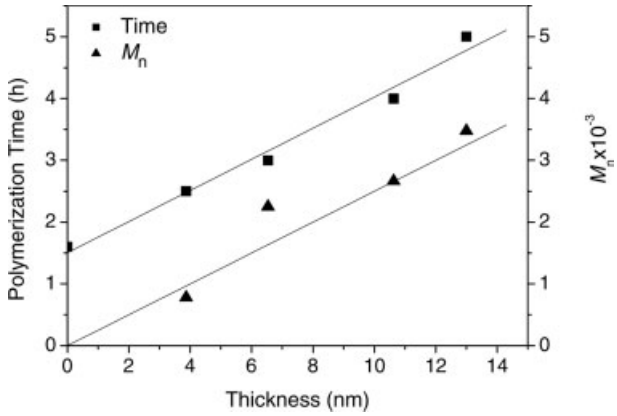

Figure 6. Dependence of (a) the thickness of the PDMAEMA layer grown from the PVDF surface by ATRP on the polymerization time and (b) the thickness of the PDMAEMA layer on M_n of the free PDMAEMA that formed in the solution.

to an induction period at the beginning of the polymerization. Figure 5(b) shows the relationship between M_n of free PDMAEMA and the conversion of the DMAEMA monomer. M_n of free PDMAEMA increased linearly with the increase in the monomer conversion. The polydispersity index [weight-average molecular weight/number-average molecular weight (M_w/M_n)] of free PDMAEMA was also around 1.1. Although the exact molecular weight of the polymer grafted onto the PVDF surface is not known, the molecular weight of the grafted polymer is expected to be proportional to that of the polymer formed in the solution.[37] These results indicate that the processes of the ATRP of DMAEMA initiated at the secondary halogenated sites of PVDF on the PVDF surface are controlled.

The ellipsometry measurements indicate a large increase in the film thickness after the growth of the PDMAEMA layer on the PVDF surface. Furthermore, because ATRP is a living polymerization process, the thickness of the polymer brushes should increase linearly with the polymerization time and the molecular weight of the graft polymer. As shown in Figure 6, an approximately linear increase in the thickness of the grafted PDMAEMA layer on the PVDF surface with the polymerization time can be observed, whereas the fitted line deviates from zero because of the induction period at the beginning of the polymerization. A linear relationship between the thickness of the PDMAEMA layer and the molecular weight of the free PDMAEMA formed in the solution can also be observed. These results indicate that the process of ATRP of DMAEMA initiated at the secondary halogenated sites of PVDF on the surface is controlled.

The changes in the topography of the PVDF surfaces after modification by surface-initiated ATRP were studied by AFM. Representative AFM images of the pristine PVDF, PVDF-*g*-PPEGMA (PPEGMA thickness = 6.4 nm), and PVDF-*g*-PDMAEMA (PDMAEMA thickness = 3.9 nm) surfaces are shown in Figure 7. The root-mean-square surface roughness of the pristine PVDF surface was only about 16.8 nm. After surface-initiated ATRP, the surface roughness decreased to about 11.0 and 9.0 nm for PVDF-*g*-PPEGMA

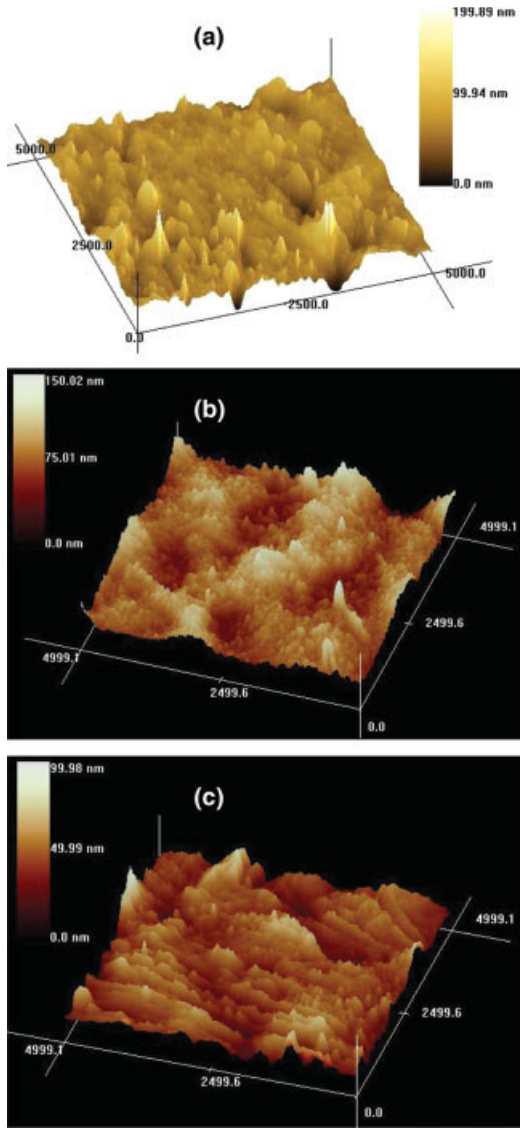

Figure 7. AFM images of (a) the pristine PVDF surface, (b) the PVDF-*g*-PPEGMA surface (PPEGMA thickness = 6.4 nm), and (c) the PVDF-*g*-PDMAEMA surface (PDMAEMA thickness = 3.9 nm).

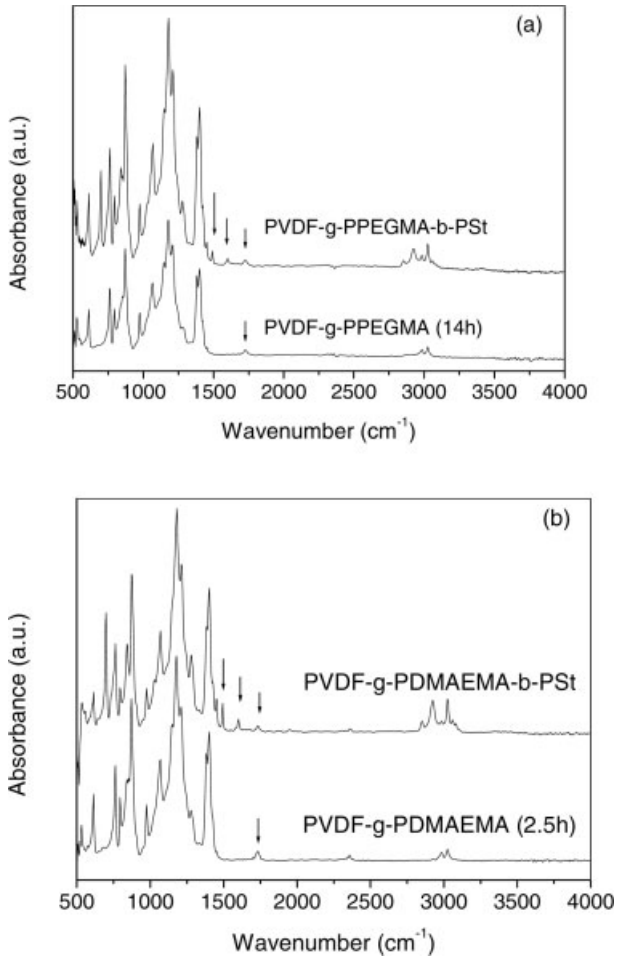

Figure 8. ATR–FTIR spectra of the PVDF surfaces with graft (a) PPEGMA-*b*-PSt and (b) PDMAEMA-*b*-PSt diblock brushes.

(PPEGMA thickness = 6.4 nm) and PVDF-*g*-PDMAEMA (PDMAEMA thickness = 3.9 nm) surfaces, respectively. These results suggest that the surface-initiated ATRP gave rise to well-defined polymer brushes and a dense coverage of polymer brushes on the PVDF surfaces. As also shown in Figure 7(b,c), the grafted polymer brushes existed as a distinctive overlayer on the PVDF surfaces. The formation of the nanosized islands probably resulted from the nanoscale phase aggregation of the grafted polymer after the surface was dried.

Diblock Polymer Brushes on PVDF Surfaces

Another advantage of ATRP over the conventional radical polymerization technique is the possibility for the synthesis of diblock copolymers. ATRP was used to synthesize the PPEGMA-*b*-PSt and PDMAEMA-*b*-PSt diblock copolymer brushes from the pristine PVDF surface. The formation of the block copolymer brushes was confirmed by ATR–FTIR and ellipsometry. A 4.2-nm increase in the thickness of the grafted polymer layer was observed by ellipsometry after the ATRP of St at 110 °C for 24 h on the PVDF-*g*-PPEGMA surface (initial thickness = 6.4 nm), whereas a 3.6-nm increase in the thickness of the grafted polymer layer was observed after the ATRP of St at 110 °C for 24 h on the PVDF-*g*-PDMAEMA surface (initial thickness = 3.9 nm). New absorption bands at 1600 and 1500 cm^{-1}, attributable to the benzene ring of the PSt block, appeared in the ATR–FTIR spectra of the PVDF-*g*-PPEGMA-*b*-PSt surface and the PVDF-*g*-PDMAEMA-*b*-PSt surface besides the absorption band at 1732 cm^{-1} attributable to the vibration of O—C=O (Fig. 8). These results confirmed that some of the dormant sites at the ends of the grafted PPEGMA and PDMAEMA chains allowed the reactivation of the graft polymerization process, resulting in the formation of the diblock copolymer brushes on the PVDF surfaces.

Antifouling Property of PVDF-*g*-PPEGMA Surfaces

The presence of hydrophilic PPEGMA brushes on the PVDF surfaces imparted significant resistance to protein adsorption. The near-surface nitrogen contents of the surfaces exposed to a 2 mg/mL BSA solution for 24 h were obtained by integration of the following peaks in the XPS survey spectra: C 1s (285 eV), N 1s (399 eV), O 1s

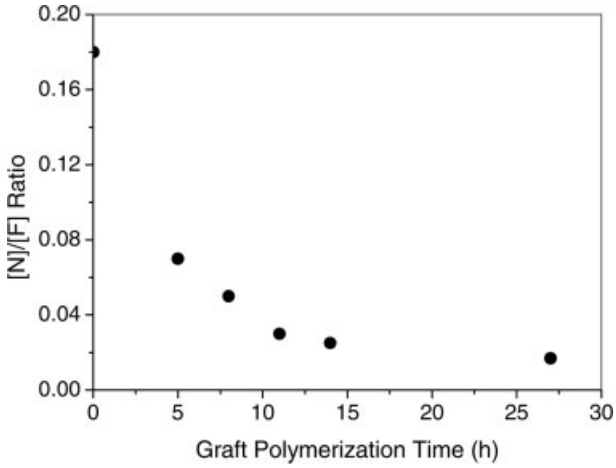

Figure 9. Dependence of the extent of BSA adsorption (expressed as the [N]/[F] ratio) on the polymerization time in the preparation of the PPEGMA-brush-grafted PVDF surface.

(531 eV), and F 1s (685 eV). The relative amount of BSA adsorbed onto the surface could be simply expressed as the [N]/[F] ratio. The dependence of the [N]/[F] ratio on the PPEGMA brushes concentration of the PVDF-*g*-PPEGMA surfaces is summarized in Figure 9. The PVDF-*g*-PPEGMA surfaces showed substantially enhanced resistance to BSA adsorption in comparison with the pristine PVDF surfaces. The PVDF surfaces with grafted PPEGMA for 5 h adsorbed BSA at a level less than 60% of that of the pristine PVDF surface, whereas graft polymerization for 27 h yielded an approximately 10-fold reduction in BSA adsorption.

CONCLUSIONS

The preparation of polymer brushes onto PVDF surfaces by ATRP initiation of methacrylic monomers at the secondary halogenated sites has been demonstrated. This technique offers an effective approach to the preparation of graft polymer brushes on PVDF surfaces, as the grafting of large proportions of the polymer chains can be accomplished without any unusual care with respect to the pretreatment of the surfaces and the purity of the reagents.

With this method, PVDF surfaces with graft PPEGMA and PDMAEMA brushes were synthesized by the graft polymerization of PEGMA and DMAEMA from the PVDF surfaces. ATR–FTIR and XPS analysis indicated the formation of polymer brushes on the PVDF surfaces. Kinetic studies revealed a linear increase in the surface coverage of the surface graft polymer brushes with the reaction time, indicating that the chain growth from the surface was a controlled process with living characteristics. Diblock copolymer brushes consisting of PPEGMA-*b*-PSt and PDMAEMA-*b*-PSt were obtained on the PVDF surfaces with either type of homopolymer brush as the macroinitiator for the ATRP of the second monomer. The homopolymer and diblock copolymer, covalently tethered to the PVDF surface, imparted new and well-structured functionalities directly onto the fluoropolymer surfaces. Protein adsorption experiments revealed that the PVDF surfaces with graft hydrophilic PPEGMA brushes had good antifouling properties.

Financial support for this work was provided by the National Natural Science Foundation of China under project number 50403016, the Scientific Research Foundation for Returned Overseas Chinese Scholars, the State Education Ministry, and the Natural Science Foundation of Jiangxi Province under project number 520044. This work made use of the experimental facilities of the Analytic Center of Nanchang University.

REFERENCES AND NOTES

1. Souzy, R.; Ameduri, B.; Boutevin, B. Prog Polym Sci 2004, 29, 75.
2. Kang, E. T.; Zhang, Y. Adv Mater 2000, 12, 1481.
3. Sacher, E. Prog Surf Sci 1994, 47, 273.
4. Pereira, N. S.; Peinemann, K. V. J Membr Sci 1992, 73, 25.
5. Flösch, D.; Lehmann, H.-D.; Reichl, R.; Inacker, O.; Göpel, W. J Membr Sci 1992, 70, 53.
6. Vestling, M. M.; Fenselau, C. Biochem Soc Trans 1994, 22, 547.
7. Speicher, D. W. Methods Enzymol 1994, 6, 262.
8. Urban, E.; King, M. W.; Guidon, R.; Laroche, G.; Marois, Y.; Martin, L.; Cardou, A.; Douville, Y. ASAIO J 1994, 40, 145.
9. Laroche, G.; Marois, Y.; Guidon, R.; King, M. W.; Martin, L.; How, T.; Douville, Y. J Biomed Mater Res 1995, 29, 1525.
10. Valentini, R. F.; Vargo, T. G.; Gardella, J. A., Jr.; Aebischer, P. J Biomater Sci Polym Ed 1993, 5, 13.
11. Costello, C. A.; McCarthy, T. J. Macromolecules 1987, 20, 2819.
12. Chan, C. M.; Ko, T. M.; Hiraoka, H. Surf Sci Rep 1996, 24, 1.
13. Griesser, H. J.; Da, Y.; Hughes, A. E.; Gengenbach, T. R.; Mau, A. W. H. Langmuir 1991, 7, 2484.
14. Golub, M. A.; Lopata, F. S.; Finney, L. S. Langmuir 1994, 10, 3629.
15. Tian, J.; Xue, Q. J. J Appl Polym Sci 1998, 69, 435.
16. Vasilets, V. N.; Hirata, I.; Iwata, H.; Ikada, Y. J Polym Sci Part A: Polym Chem 1998, 36, 2215.
17. Mathieson, I.; Brewis, D. M.; Sutherland, I.; Cayless, R. A. J Adhes 1994, 46, 49.
18. Boutevin, B.; Robin, J. J.; Serdani, A. Eur Polym J 1992, 28, 1507.
19. Everett, M. L.; Hoflund, G. B. J Polym Sci Part A: Polym Chem 2005, 43, 552–561.
20. Ogoshi, T.; Chujo, Y. J Polym Sci Part A: Polym Chem 2005, 43, 3543–3550.
21. Zhao, B.; Brittain, W. J. Prog Polym Sci 2000, 25, 667.
22. Kato, K.; Uchida, E.; Kang, E. T.; Uyama, Y.; Ikada, Y. Prog Polym Sci 2003, 28, 209.
23. Uyama, Y.; Kato, K.; Ikada, Y. Adv Polym Sci 1998, 137, 1.
24. Tan, K. L.; Woon, L. L.; Wong, H. K.; Kang, E. T.; Neoh, K. G. Macromolecules 1993, 26, 2832.
25. Inagaki, N.; Tasaka, S.; Goto, Y. J Appl Polym Sci 1997, 66, 77.

26. Yang, M. R.; Chen, K. S. Mater Chem Phys 1997, 50, 11.
27. Becker, W.; Bothe, M.; Schmidt-Naake, G. Angew Makromol Chem 1999, 273, 57.
28. Akinay, E.; Tincer, T. J Appl Polym Sci 2001, 79, 816.
29. Konig, U.; Nitschke, M.; Menning, A.; Eberth, G.; Pilz, M.; Arnhold, C.; Simon, F.; Adam, G.; Werner, C. Colloids Surf B 2002, 24, 63.
30. Li, J. Y.; Sato, K.; Ichiduri, S.; Asano, S.; Ikeda, S.; Iida, M.; Oshima, A.; Tabata, Y.; Washio, M. Eur Polym J 2004, 40, 775.
31. Edmondson, S.; Osborne, V. L.; Huck, W. T. S. Chem Soc Rev 2004, 33, 14.
32. Hawker, C. J.; Wooley, K. L. Science 2005, 309, 1200.
33. Hawker, C. J.; Bosman, A. W.; Harth, E. Chem Rev 2001, 101, 3661.
34. Matyjaszewski, K.; Xia, J. Chem Rev 2001, 101, 2921.
35. Kamigaito, M.; Ando, T.; Sawamoto, M. Chem Rev 2001, 101, 3689.
36. Chiefari, J.; Chong, Y. K.; Ercole, F.; Krstina, J.; Jeffery, J.; Le, T. P. T.; Mayadunne, R. T. A.; Meijs, G. F.; Moad, C. L.; Moad, G.; Rizzardo, E.; Thang, S. H. Macromolecules 1998, 31, 5559.
37. Ejaz, M.; Yamamoto, S.; Ohno, K.; Tsujii, Y.; Fukuda, T. Macromolecules 1998, 31, 5934.
38. Husseman, M.; Malmström, E. E.; McNamara, M.; Mate, M.; Mecerreyes, D.; Benoit, D. G.; Hedrick, J. L.; Mansky, P.; Huang, E.; Russell, T. P.; Hawker, C. J. Macromolecules 1999, 32, 1424.
39. Matyjaszewski, K.; Miller, P. J.; Shukla, N.; Immaraporn, B.; Gelman, A.; Luokala, B. B.; Siclovan, T. M.; Kickelbick, G.; Vallant, T.; Hoffmann, H.; Pakula, T. Macromolecules 1999, 32, 8716.
40. Mori, H.; Boker, A.; Krausch, G.; Müller, A. H. E. Macromolecules 2001, 34, 6874.
41. Tsujii, Y.; Ejaz, M.; Sato, K.; Goto, A.; Fukuda, T. Macromolecules 2001, 34, 8872.
42. Baum, M.; Brittain, W. J. Macromolecules 2002, 35, 610.
43. Zheng, G. D.; Stöver, H. D. H. Macromolecules 2003, 36, 1808.
44. Edmondson, S.; Huck, W. T. S. J Mater Chem 2004, 14, 730.
45. Granville, A. M.; Boyes, S. G.; Akgun, B.; Foster, M. D.; Brittain, W. J. Macromolecules 2004, 37, 2790.
46. Yu, W. H.; Kang, E. T.; Neoh, K. G.; Zhu, S. J Phys Chem B 2003, 107, 10198.
47. Khan, M.; Huck, W. T. S. Macromolecules 2003, 36, 5088.
48. Feng, W.; Brash, J.; Zhu, S. J Polym Sci Part A: Polym Chem 2004, 42, 2931–2942.
49. Reddy, S. K.; Sebra, R. P.; Anseth, K. S.; Bowman, C. N. J Polym Sci Part A: Polym Chem 2005, 43, 2134–2144.
50. Bian, K.; Cunningham, M. F. J Polym Sci Part A: Polym Chem 2005, 43, 2145–2154.
51. Liu, T.; Casado-Portilla, R.; Belmont, J.; Matyjaszewski, K. J Polym Sci Part A: Polym Chem 2005, 43, 4695–4709.
52. Gravano, S. M.; Dumas, R.; Liu, K.; Patten, T. E. J Polym Sci Part A: Polym Chem 2005, 43, 3675–3688.
53. Kotal, A.; Mandal, T. K.; Walt, D. R. J Polym Sci Part A: Polym Chem 2005, 43, 3631–3642.
54. Moine, L.; Deleuze, H.; Degueil, M.; Maillard, B. J Polym Sci Part A: Polym Chem 2004, 42, 1216–1226.
55. Zhao, H.; Argoti, S. D.; Farrell, B. P.; Shipp, D. A. J Polym Sci Part A: Polym Chem 2004, 42, 916–924.
56. Beers, K. L.; Gaynor, S. G.; Matyjaszewski, K. Macromolecules 1998, 31, 9413–9415.
57. Gu, L.; Zhu, S.; Hrymak, A. N. J Polym Sci Part B: Polym Phys 1998, 36, 705.
58. Paik, H.-J.; Gaynor, S. G.; Matyjaszewski, K. Macromol Rapid Commun 1998, 19, 47–52.
59. Hester, J. F.; Banerjee, P.; Won, Y.-Y.; Akthakul, A.; Acar, M. H.; Mayes, A. M. Macromolecules 2002, 35, 7652–7661.